Original scientific paper
Journal of Central European Agriculture, 2022, 23(3), p.552-563
DOI: /10.5513/JCEA01/23.3.3515

Model for estimating barley production based on satellite images

Model de estimare a producției de orz pe baza imaginilor satelitare

Florin SALA[1], Mihai Valentin HERBEI[2] (✉)

[1] Banat University of Agricultural Sciences and Veterinary Medicine "King Michael I of Romania" from Timisoara, Soil Science and Plant Nutrition, 119 Calea Aradului, 300645, Timisoara, Romania

[2] Banat University of Agricultural Sciences and Veterinary Medicine "King Michael I of Romania" from Timisoara, Remote Sensing and GIS, 119 Calea Aradului, 300645, Timisoara, Romania

✉ Corresponding author: mihai_herbei@yahoo.com

Received: January 19, 2022; accepted: May 16, 2022

ABSTRACT

The present study aimed to analyze and evaluate the barley crops, and also to estimate production by analyzing satellite images. The study was conducted at Didactic and Experimental Resort (DER) of BUASVM Timisoara, Timis County, Romania. The PlanetScope platform was used for the study, with a spatial resolution of 3 m. The satellite images were taken in the PlanetScope Remote Sensing System, at 7 different moments, between 27 March and 27 June 2020. Based on spectral data, MSAVI2 and NDVI indices were calculated. Four plots cultivated with barley were studied (B/A75, B/A80, B/A82 and B/A84). The variation of the MSAVI2 and NDVI indices in relation to the time factor (T, days), over the study interval, was described by the polynomial models of 2nd degree, in statistical accuracy conditions. Based on the regression analysis, the estimation of the production based on the MSAVI2 and NDVI indices was possible under the conditions of R^2=0.998, P<0.05 for plot B/A75, R^2=0.999, P<0.05 for plot B/A80, R^2=0.997, P=0.0577 for plot B/A82 and respectively, R^2=0.999, P<0.05 for plot B/A84. From the calculation of the RMSEP index, for the estimated productions, the values were obtained: RMSEP=80.8162 for $Y_{B/A75}$, RMSEP=50.1633 for $Y_{B/A80}$, RMSEP=192.3947 for $Y_{B/A82}$ and respectively RMSEP=112.2899 for $Y_{B/A84}$. The value of RMSEP=50.1633 for $Y_{B/A80}$ confirms that for the plot B/A80 the production estimate was made with the highest precision.

Keywords: barley, PlanetScope, prediction model, satellite imagery, yield

ABSTRACT

Prezentul studiu a avut ca scop analiza și evaluarea culturilor de orz, precum și estimarea producției prin analiza imaginilor satelitare. Studiul a fost realizat la Statiunea Didactica si Experimentala (SDE) a BUASVM Timisoara, Judetul Timis, Romania. Pentru studiu a fost utilizată platforma PlanetScope, cu o rezoluție spațială de 3 m. Imaginile satelitare au fost realizate în Sistemul de Teledetecție PlanetScope, în 7 momente diferite, în perioada 27 March and 27 June 2020. Pe baza datelor spectrale, au fost calculați indicii MSAVI2 și NDVI. Au fost studiate patru parcele cultivate cu orz (B/A75, B/A80, B/A82 si B/A84). Variația indicilor MSAVI2 și NDVI în raport cu factorul timp (T, zile), pe intervalul de studiu, a fost descrisă de modelele polinomiale de gradul II, în condiții de acuratețe statistică. Pe baza analizei de regresie, estimarea producției pe baza indicilor MSAVI2 și NDVI a fost posibilă în condițiile R^2=0,998, P<0,05 pentru parcela B/A75, R^2 =0,999, P<0,05 pentru parcela B/A80, R^2=0,997, P=0,0577 pentru parcela B/A82 și respectiv, R^2 =0,999, P<0.05 pentru parcela B/A84. Din calculul indicelui RMSEP, pentru producțiile estimate, s-au obținut valorile: RMSEP =80,8162 pentru $Y_{B/A75}$, RMSEP =50,1633 pentru $Y_{B/A80}$, RMSEP=192,3947 pentru $Y_{B/A82}$ și respectiv RMSEP =112.2899 pentru $Y_{B/A84}$. Valoarea RMSEP =50,1633 pentru $Y_{B/A80}$ confirmă faptul că pentru parcela B/A80 estimarea producției a fost făcută cu cea mai mare precizie.

Cuvinte cheie: orz, PlanetScope, model predicție, imagini satelitare, producție

DOI: /10.5513/JCEA01/23.3.3515

INTRODUCTION

The concern of the people to manage the agricultural crops has a permanent character, and the methods of approach have diversified and developed in time, from simple observations to extremely precise analysis and predictions (Spiertz, 2013; Nuruzzaman et al., 2019; Sharma et al., 2019; Kaur et al., 2020; Miner et al., 2020). Techniques based on satellite imagery and imaging analysis for the study of terrestrial areas and agricultural crops offer numerous advantages for different types of agricultural systems (Khanal et al., 2020; Sishodia et al., 2020; Jurišić et al., 2021; Mulla, 2021). Cereal crops are of great importance in agricultural systems and for food security (Shiferaw et al., 2013; García et al., 2020). Barley is one of the ancient agricultural crops of the people. Barley culture, based on its importance, has been studied from socio-economic, educational, food security perspectives, as well as in relation to different categories of conditions and influencing factors (Newton et al., 2011; Langridge, 2018; Hkurunziza et al., 2020; Sakellariou and Mylona, 2020). By methods based on satellite and aerial or terrestrial images, agricultural crops were analyzed and evaluated in relation to physiological indices (Mourad et al., 2020; Mzid et al., 2020), the expression of genotypes or cultures (Kefauver et al., 2017), the effect of fertilizers (Bu et al., 2017), crop irrigation and water use efficiency (Tedese et al., 2015; Vuolo et al., 2015), the response of plants to various stressors (Khanal et al., 2020), production and quality (Bu et al., 2017; Panek and Gozdowski, 2020). Modeling offers the facility to quantitatively predict agricultural production, or quality elements of it, based on directly quantifiable elements (inputs: production factors - fertilizer doses, volume of irrigation water, phytosanitary treatments, etc.) (Wagner et al., 2007; van Klompenburg et al., 2020; Shahhosseini et al., 2021), or indirectly through spectral information from satellite images and calculated specific indices (Tan et al., 2020; Zhang et al., 2020; Zhao et al., 2020). Remote sensing techniques have made it easier to calculate and use different indices (eg. NDVI, NBR, SAVI, MCARI, MSAVI, TCARI, etc.) based on spectral information in images to characterize the soil (Nguyen et al., 2021), vegetal cover (Xue and Su, 2017), agricultural crops (Ulfa et al., 2022), crop nutrition (Sharifi, 2020), plant stress (Galieni et al., 2021), biomass production (Kumar et al., 2015; Geng et al., 2021) and other useful aspects for farm management. Very important is the ease of estimating the production of different crops based on indices resulting from the technique based on remote sensing (Khalil and Abdullaev, 2021; Ji et al., 2021; Zhu et al., 2021; Ulfa et al., 2022) . This facilitates the establishment of the harvesting moment, the organization of the harvesting, the transport and storage of the production, the capitalization on the market. Validation of crop analysis and estimation models based on satellite images through biomass production or grain production, leads to obtaining models with high precision and also with extended applicability (Noureldin et al., 2013; Shiu and Chuang, 2019; Zhao et al., 2020). The present study used satellite imagery, the PlanetScope platform, to analyze barley crops and estimate barley grain production.

MATERIAL AND METHODS

The study aimed to evaluate barley crops and estimate barley production based on satellite images, the PlanetScope platform, and remote sensing resources.

Study area

The study was carried out within Didactic and Experimental Resort (DER) of BUASVM Timisoara, Timiș County, Romania (Figure 1). Four plots cultivated with barley were studied (B/A75 with surface of 52.32 ha; B/A80 with surface of 54.49 ha; B/A82 with surface of 53.96 ha; B/A84 with surface of 52.22 ha).

Cultivation conditions

The soil is of the chernozem type, with some gleic properties in plot A84 and some micro areas (unevenly distributed) with saline influences on plots A75 and A82. The sunflower was the previous crop plant, and the agro technical works were applied similarly, for all four plots. The land was prepared for sowing through the disc works. Complex fertilizers (18:46:0), in a dose of 150 kg ha^{-1}, were applied before sowing, when preparing the

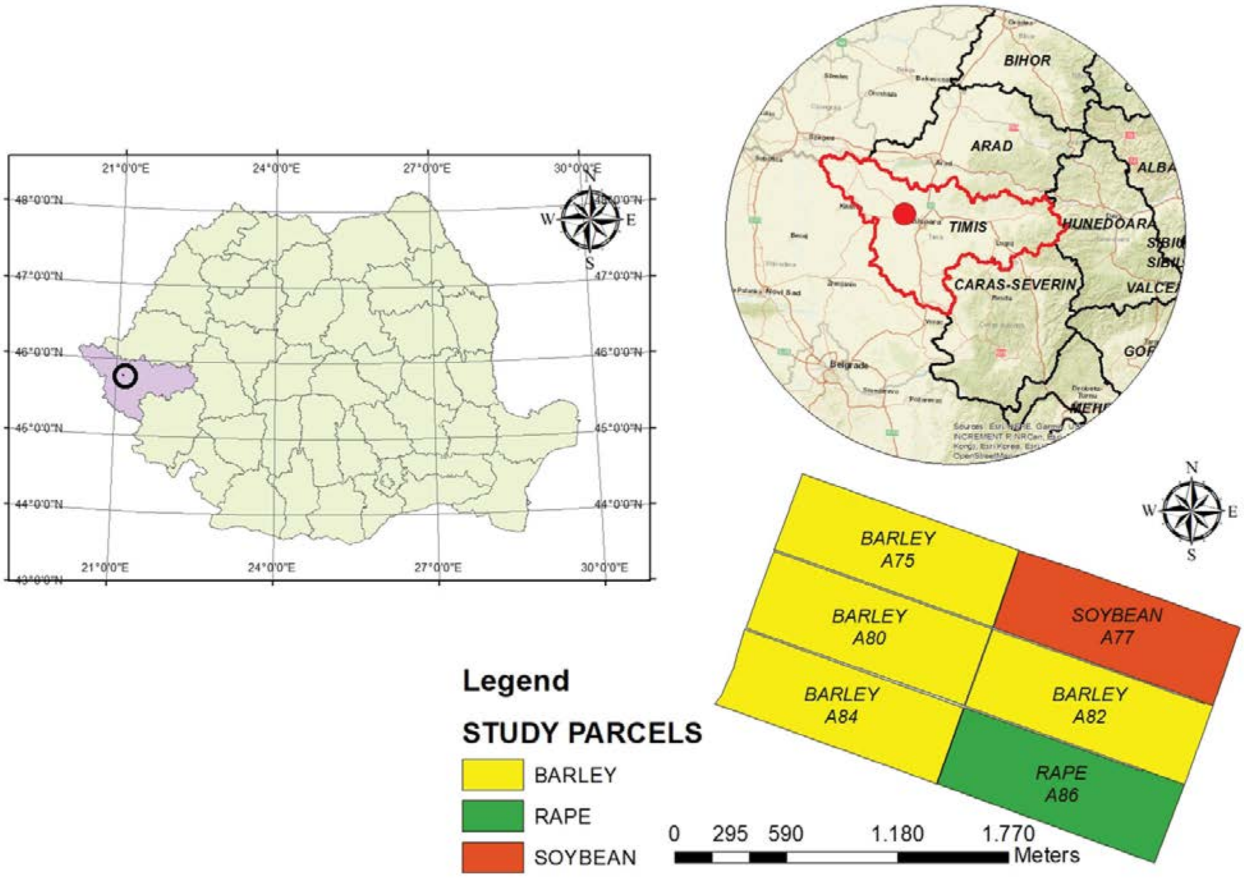

Figure 1. Location of the study area, BUASVM Timisoara, Timis County, Roma

soil. Nitrogen fertilizers (urea, 200 kg ha^{-1}) were applied in vegetation (spring 2020). In the vegetation period, a herbicide treatment was done (Rival 75 product), and two fungal treatments (Falcon product). The cultivated barley variety was Atlantic.

Remote Sensing Data

In the present study, satellite images used were taken from the portal www.planet.com, which offers a wide variety of remote sensing products. The PlanetScope platform was used for the study, with a spatial resolution of 3 m and which captures scenes in four spectral bands with different characteristics (Table 1).

PlanetScope images have a scene footprint of approx. 24.4 km × 8.1 km, and the satellites capture scenes after an interval of about one second, resulting in a small overlap between consecutive scenes. The PlanetScope mission currently consists of about 140 small cube satellites, operating in low-earth sun-synchronous orbits

Table 1. Characteristics of spectral bands, PlanetScope

Band No.	Description	Wavelength (μm)	Spatial resolution (m)
Band 1	Blue	0.455 – 0.515	
Band 2	Green	0.500 – 0.590	3
Band 3	Red	0.590 – 0.670	
Band 4	Near-Infrared	0.780 – 0.860	

with a daily revisit time or lower, resulting in one image of every part of the landmass of the earth at least once a day. The satellite images were taken in the PlanetScope Remote Sensing System, at different dates, in the interval 27 March and 27 June 2020. Based on spectral data, the indices MSAVI2, relation (1) and NDVI, relation (2), Qi et al. (1994), Rouse et al. (1973), were calculated (Figure 2 and Figure 3).

$$\text{MSAVI2} = \frac{2NIR+1-\sqrt{(2NIR+1)^2-8(NIR-RED)}}{2} \quad (1)$$

$$\text{NDVI} = \frac{NIR-RED}{NIR+RED} = \frac{BAND4-BAND3}{BAND4+BAND3} \quad (2)$$

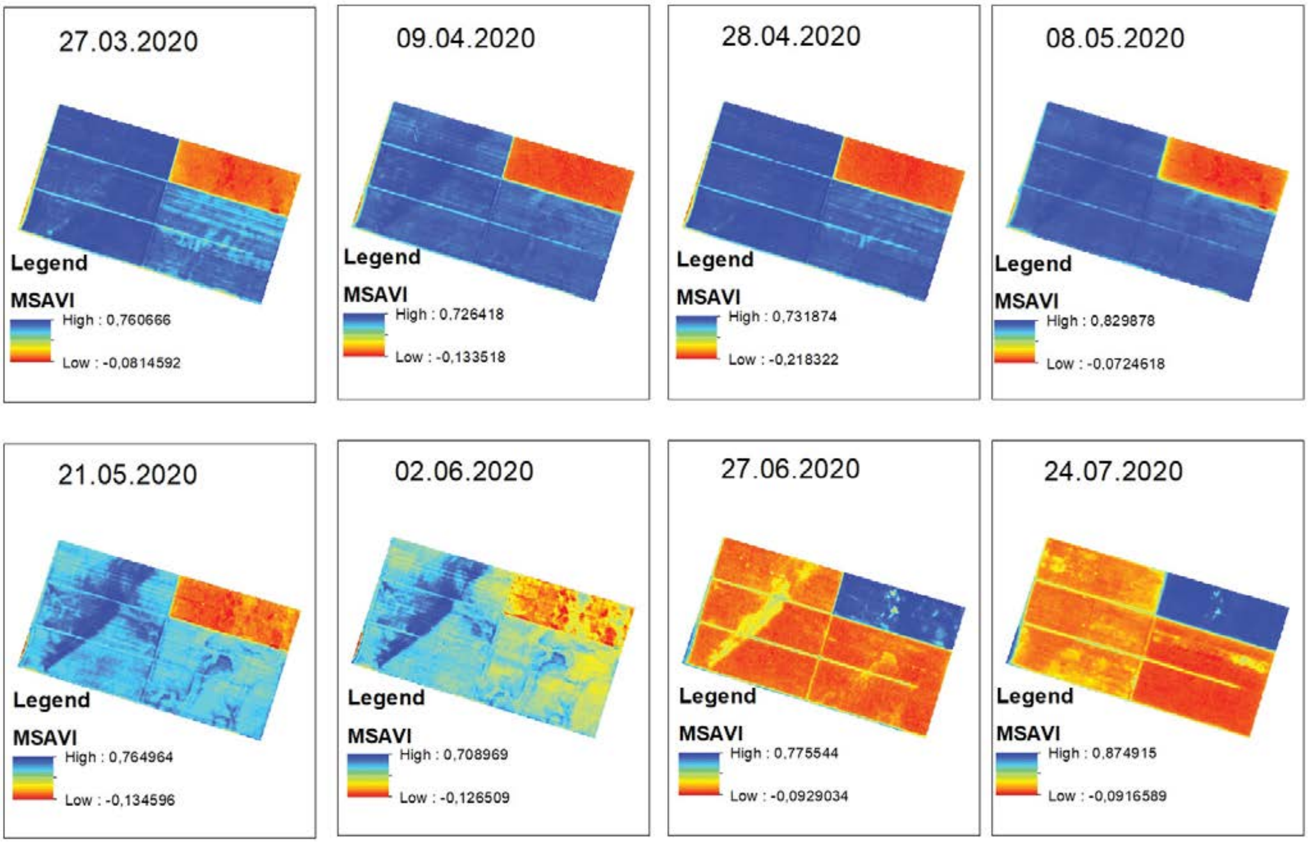

Figure 2. MSAVI2 maps for barley plots during the study period

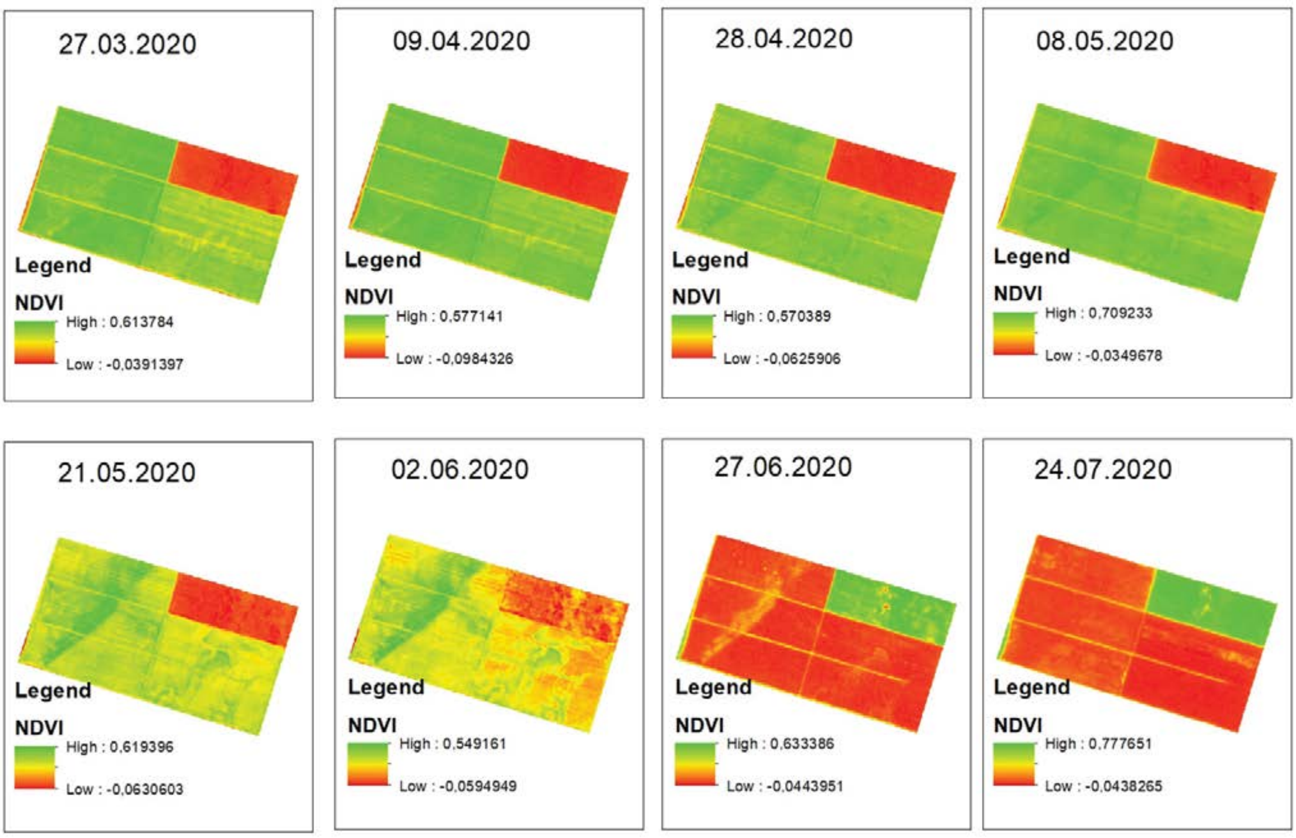

Figure 3. NDVI maps for barley plots during the study period

Statistical analysis

The data obtained for the MSAVI2 and NDVI indices were analyzed in relation to the productions obtained, in terms of the level of correlation. To obtain models for estimating production based on the values of the MSAVI2 and NDVI indices, regression analysis was used. The estimation of the safety of the results was evaluated based on the regression coefficients R^2, of the parameter p. Based on the ANOVA test, the safety of the coefficients of the functions obtained for estimating the barley production at the level of the studied plots was evaluated. The logical scheme of the working model is presented in Figure 4. ArcGIS v.10.6 software was used for satellite image processing (ESRI, 2011), and EXCEL analysis module and PAST software were used for data analysis and processing (Hammer et al., 2001). Wolfram Alpha (2020) software was used to generate 3D and isoquants graphics.

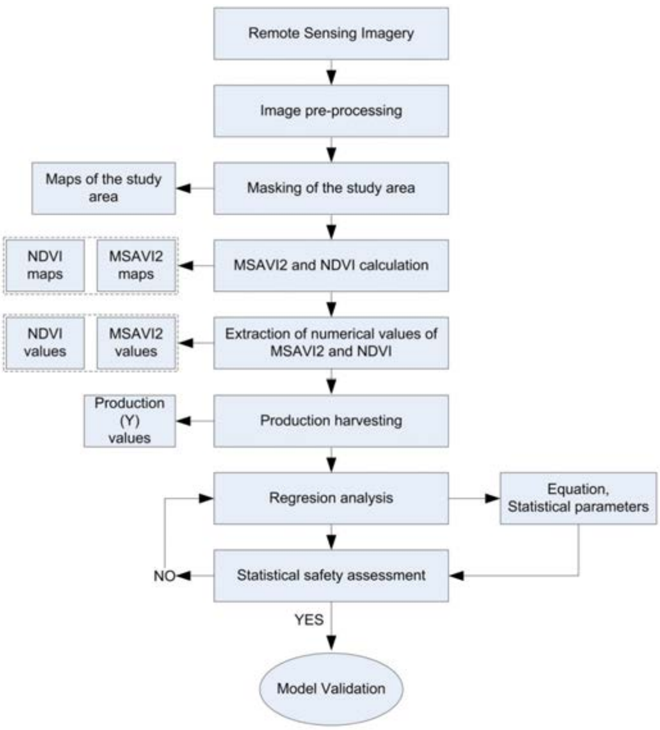

Figure 4. The logical scheme of the working model

RESULTS

From the analysis of the satellite images taken at 7 staggered moments during the vegetation period of the barley crop, spectral information resulted based on which the MSAVI2 and NDVI indices were calculated, table 2. The correlation analysis of the values of MSAVI2 and NDVI indices with time, during the study period, showed strong and moderate correlations. Thus, in the case of MSAVI2 vs. T, strong negative correlations were registered, corresponding to plots B/A75 (r=-0.823) and B/A84 (r=-0.811) and moderate negative correlations at the level of plots B/A80 (r =-0.768) and B/A82 (r=-0.788).

Similar correlation levels were identified in the case of the NDVI index, respectively strong negative correlations on plot B/A75 (r=-0.826) and on plot B/A84 (r=-0.814), and moderate correlations on plot B/A80 (r=-0.764) and B/A82 (r=-0.760). Moderate correlations were found between production (Y) and MSAVI2 for the period 27 March – 09 April (r=0.734, r=0.759), and between production (Y) and NDVI were found similar, moderate positive correlations for the same period (r=0.737, r=0.770). During the study period, a variation of the values of the MSAVI2 and NDVI indices was registered, associated with the vegetal cove of the barley culture studied at the level of the four plots. The variation of the MSAVI2 index in relation to the time factor (T, days), between the image capture moments, was described by polynomial models of 2nd degree, in statistical accuracy conditions (R^2 =0.933, P<0.01; F=27.847 for plot B/A75; R^2=0.934, P<0.01; F=28.291 for plot B/A80; R^2=0.938, P<0.01; F=30.198 for plot B/A82; R^2=0.933, P<0.01; F=27.894 for plot B/A84). The variation of the NDVI index in relation to the time factor (T, days) was described by polynomial models of 2nd degree, in conditions of statistical accuracy (R^2=0.893, P<0.05; F=16.692 for plot B/A75; R^2=0.898, P<0.05; F=17.682 for plot B/A80; R^2=0.875, P<0.05; F=14.056 for plot B/A82; R^2=0.890, P<0.05; F=16.183 for plot B/A84). A model of the graphical distribution of the MSAVI2 index according to the time factor (T), at the level of plot B/A82, is described by equation (3), it is shown in Figure 5.

Table 2. Values of calculated indices and barley production over the study interval

Indices	Time	Plots no			
		B/A75	B/A80	B/A82	B/A84
MSAVI2 – 27 March	t1	0.6958866	0.6786077	0.5951841	0.6854168
NDVI – 27 March		0.5352913	0.5158649	0.4250858	0.5243227
MSAVI2 – 09 April	t2	0.6573405	0.6518728	0.5956254	0.6544560
NDVI – 09 April		0.4913397	0.4859226	0.4252220	0.4895524
MSAVI2 – 28 April	t3	0.6118279	0.6370110	0.5961876	0.6123887
NDVI – 28 April		0.4424532	0.4695009	0.4254455	0.4430374
MSAVI2 – 08 May	t4	0.7437536	0.7634250	0.7191324	0.7488148
NDVI – 08 May		0.5932253	0.6190090	0.5622343	0.6002673
MSAVI2 – 21 May	t5	0.5723343	0.6047407	0.5061513	0.5637195
NDVI – 21 May		0.4048098	0.4367038	0.3406261	0.3946720
MSAVI2 – 02 June	t6	0.4837335	0.5271278	0.3946661	0.4866323
NDVI – 02 June		0.3236167	0.3613339	0.2485543	0.3239888
MSAVI2 – 27 June	t7	0.1088190	0.1006664	0.0680929	0.0867646
NDVI – 27 June		0.0595338	0.0561220	0.0364383	0.0487209
Y (kg ha^{-1})		4400	4500	4000	5000

$$MSAVI2 = -0.0001301x^2+0.006423x+0.5722 \quad (3)$$

where: x – time T (days).

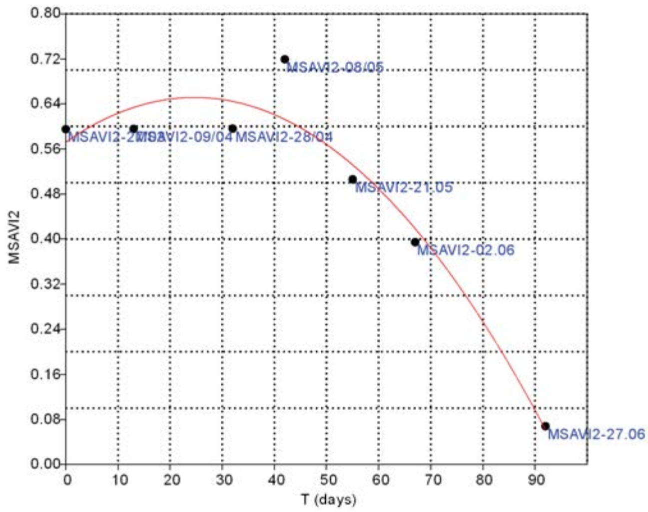

Figure 5. Graphic distribution of MSAVI2 values in relation to the time factor (T), plot B/A82

The regression analysis assessed the possibility of predicting barley production based on the MSAVI2 and NDVI indices. A model was obtained, of the type of equation (4), which described the variation of production in relation to the MSAVI2 and NDVI indices, and the values of the coefficients of the equation, for each plots studied, are shown in Table 3.

$$Y=ax^2+by^2+cx+dy+exy+f \quad (4)$$

In the case of plot B/A75, according to equation (4) was obtained the estimation of barley production in statistical safety conditions, according to R^2=0.998, P=0.022. The graphical distribution in 3D and isoquants form of the production (Y) in relation to MSAVI2 (x-axis) and NDVI (y-axis) is shown in Figure 6 (a and b).

In the case of plot B/A80, according to equation (4) was obtained the estimation of barley production in statistical safety conditions, according to R^2=0.999, P=0.0133.

DOI: /10.5513/JCEA01/23.3.3515

Table 3. Values of calculated indices and barley production over the study interval

Equation (4) coefficients values	Plots no			
	B/A75	B/A80	B/A82	B/A84
a	-745212.51827625	-751628.192773906	-1459592.60064914	-1498494.61703912
b	-903897.25745277	-885083.485199519	-2001019.31033495	-1867565.88592391
c	190595.836074336	123292.731742635	375359.790847428	474640.127899899
d	-256548.420810244	-117682.28018662	-579630.662983587	-729687.371104365
e	1688765.87665082	1609101.135485	3579556.69276343	3561167.11185397
f	0	0	0	0

Note: f is the Intercept coefficient in Equation (4), resulting from the Regression Analysis, in conditions of Constant is Zero, and Confidence Level: 95%.

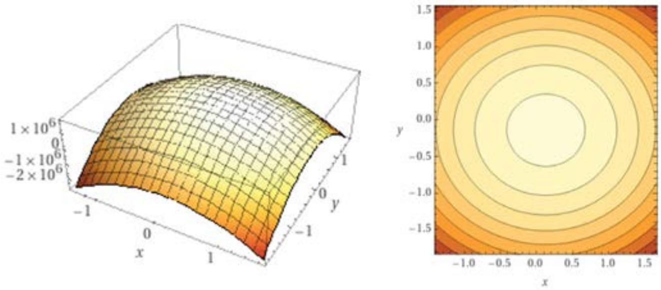

Figure 6. Graphic distribution of barley production, plot B/A75: (a) 3D distribution of barley production according to MSAVI2 and NDVI; (b) Distribution in isoquants form of barley production according to MSAVI2 and NDVI

The graphical distributions of the production (Y), in 3D form and in the form of isoquants, in relation to MSAVI2 (x-axis) and NDVI (y-axis), is shown in Figure 7 (a and b).

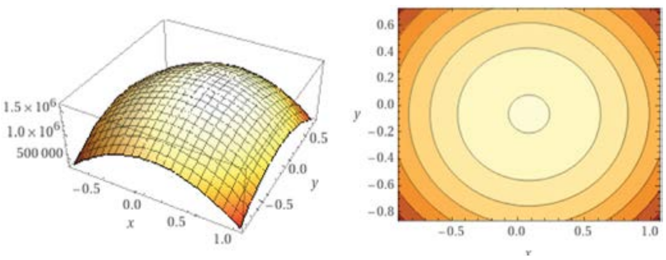

Figure 7. Graphic distribution of barley production, plot B/A80: (a) 3D distribution of barley production according to MSAVI2 and NDVI; (b) Distribution in isoquants form of barley production according to MSAVI2 and NDVI

In the case of plot B/A82, according to equation (4) was obtained the estimation of barley production in statistical safety conditions, according to R^2=0.997, P=0.0577. The graphical distributions of the production variation (Y) in 3D form and in the form of isoquants, in relation to MSAVI2 (x-axis) and NDVI (y-axis), is shown in Figure 8 (a), and (b).

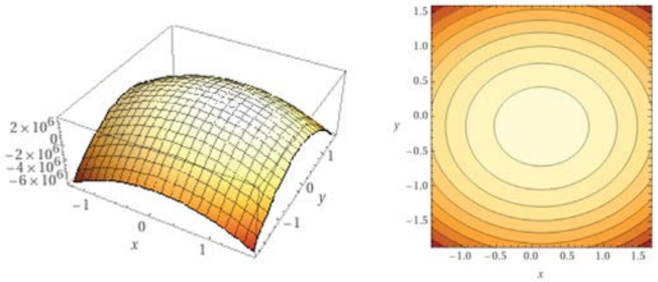

Figure 8. Graphic distribution of barley production, plot B/A82: (a) 3D distribution of barley production according to MSAVI2 and NDVI; (b) Distribution in isoquants form of barley production according to MSAVI2 and NDVI

In the case of plot B/A84, according to equation (4) was obtained the estimation of barley production in statistical safety conditions, according to R^2=0.999, P=0.0269. Graphical distributions of the production variation (Y), in 3D form and in isoquants form, in relation to MSAVI2 (x-axis) and NDVI (y-axis), is shown in Figure 9 (a and b).

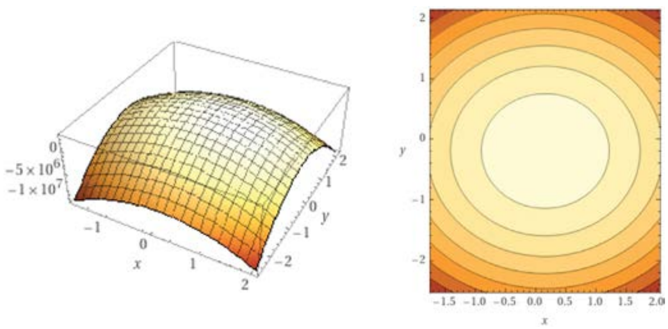

Figure 9. Graphic distribution of barley production, plot B/A84: (a) 3D distribution of barley production according to MSAVI2 and NDVI; (b) Distribution in isoquants form of barley production according to MSAVI2 and NDVI

The analysis of the estimated production differences based on the MSAVI2 and NDVI indices in relation to the average production obtained on each of the 4 plots studied, in relation to the date when the satellite images were taken, led to obtaining estimation errors (Table 4, Figure 10). In relation to the date of registering the images, it was found that the lowest average values of errors were recorded based on the images taken at time t4 (08 May), when barley crops most accurately expressed the state of vegetation. In relation to the analyzed plot, the smallest errors were registered for plot B/A80 (Table 4, Figure 10). The resulting diagram based on PCA captured the distribution of MSAVI2 and NDVI indices calculated based on satellite images, in relation to the t (t1 - t7) image acquisition moments, respectively with the spectral information contained for the four plots cultivated with barley (Figure 11). PC1 explained 99.441% of variance, and PC2 explained 0.38795% of variance.

Table 4. Average errors between Y estimated based on the MSAVI2 and NDVI indices and the average real production

Image capture time		Production prediction errors on plots			
Date	time	B/A75	B/A80	B/A82	B/A84
27 March	t1	-98.6452	-90.589	-26.5429	-137.821
09 April	t2	-49.4614	-3.0505	-76.3539	32.95629
28 April	t3	50.31222	65.46284	-132.099	-34.4548
08 May	**t4**	**53.37012**	**15.20072**	**32.67469**	**48.51497**
21 May	t5	133.6856	53.92233	405.3632	213.8595
02 June	t6	-99.3508	-43.9041	-242.597	-134.404
27 June	t7	20.48002	6.871991	104.3324	29.00245

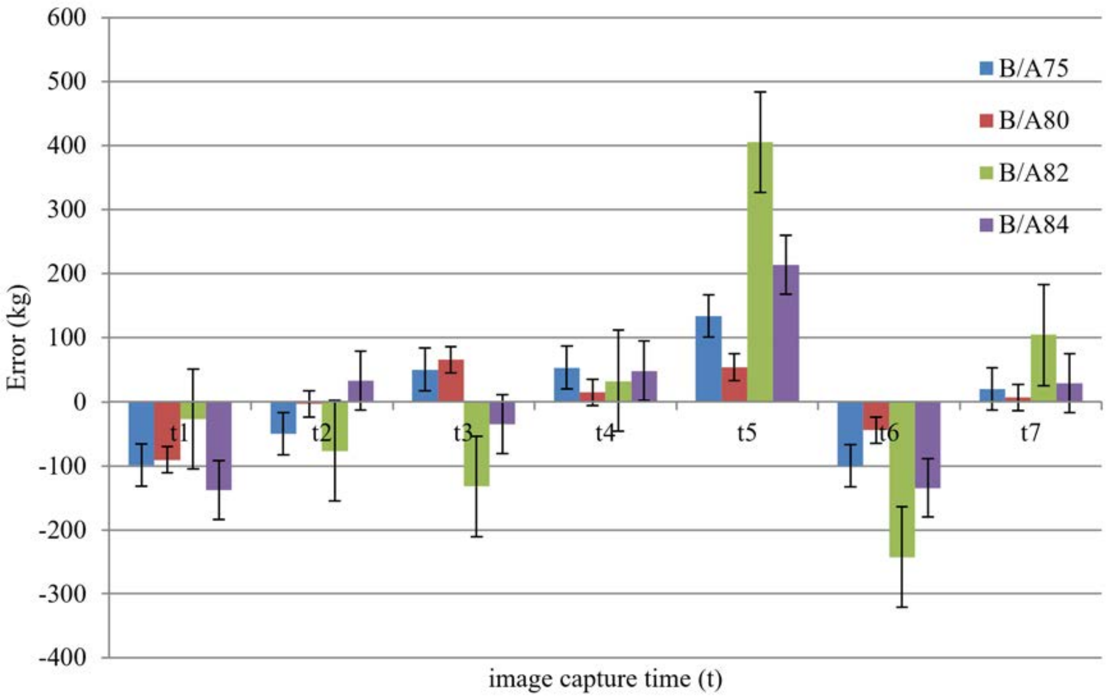

Figure 10. Graphic distribution of prediction errors of barley production, on the study plots

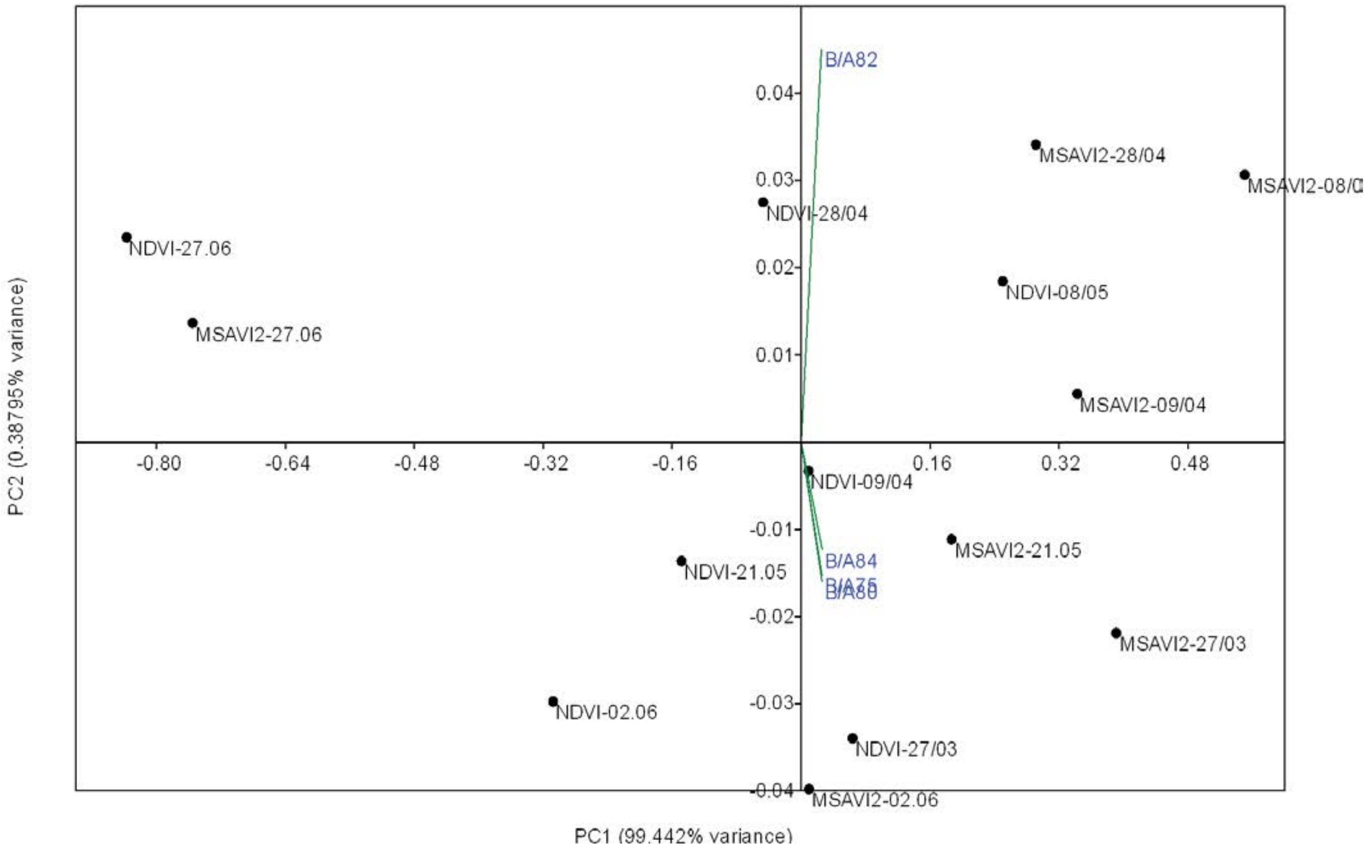

Figure 11. PCA diagram with the distribution of MSAVI2 and NDVI indices in relation to the t-moments of image capture

DISCUSSION

During the study period, the temporal variability (on the 7 study moments) and the spatial variability of the cultures (on the 4 plots) were registered. The coefficient of variation (CV) for the MSAVI2 index, in relation to the four plots, registered values between CVMSAVI2=38.3988 for B/A80, and CVMSAVI2=42.9728 for B/A82. In relation to the study moments (t1 - t7), the CV values registered values between CVt4=2.47762 in case of t4 moment and CVt7=19.57367 in case of t7 moment.

The coefficient of variation (CV) for the NDVI index registered values between CVNDVI=42.4958 in the case of plot B/A80 and CVNDVI=47.9264 in the case of plot B/A82. In relation to the study moments (t1 - t7), the CV index registered values between CVt4=3.97887 and CVt7 =20.37058. Estimation of barley production for the four plots under study was possible based on the MSAVI 2 and NDVI indices calculated from the spectral information of the satellite images, the PlanetScope product, in statistical accuracy conditions. From the analysis of the values of the regression coefficients (R^2) and of the RMSEP values, the different accuracy of the production prediction models was found. Thus, from the analysis of the RMSEP index, for the estimated productions, the values were obtained: RMSEP=80.8162 for $Y_{B/A75}$, RMSEP=50.1633 for $Y_{B/A80}$, RMSEP=192.3947 for $Y_{B/A82}$ and respectively RMSEP=112.2899 for $Y_{B/A84}$. The value of RMSEP=50.1633 for $Y_{B/A80}$ confirms that for plot B/A80 the production estimate was made with the highest precision. This reveals a plot with a uniform culture, with a reduced spatial variability. The values of the CV variation coefficient, in relation to the 4 studied plots and 7 study moments, highlighted the spatial and temporal variation of the barley crops.

Spatial variability of crops and production has been studied and confirmed in other studies, in relation to indices calculated based on satellite images, in relation to climatic conditions, soil, nutrients or stressors (Ali et al., 2019; Brogi et al., 2020; Cammarano et al., 2020). High accuracy in evaluating the production prediction for grass grain crops, assessed on the basis of dedicated statistical indices (R^2, RMSE, RMSEP), were reported for wheat (Meroni et al., 2013; Śatir and Berberoglu, 2016; Zhang et al., 2020; Zhao et al., 2020; Sharifi, 2021), barley (Hansen et al., 2002; Paudel et al., 2021), maize (Joshi et al., 2019; Jeffries et al., 2020), potato (Gómez et al., 2019), soybean (Maimaitijiang et al., 2020), sunflower (Trepos et al., 2020), but also other crops. Meroni et al. (2013) reported high safety in estimating wheat production based on remote sensing (R^2 up to 0.8). High levels of safety have been reported in other studies in estimating wheat production, R^2=0.74 and R^2=0.81 (Zhang et al., 2020). Zhao et al. (2020) reported values of the safety level in estimating wheat production based on OSAVI index at the level of R^2=0.74, respectively at the level of R^2 over 0.9 when using OSAVI index combined with other plant indices. In studies on the prediction of production of wheat, corn and cotton on large areas (thousand ha), Śatir and Berberoglu (2016) reported that the level of statistical safety was lower (R^2 adj. 0.46 to 0.65).

The results recorded in the present study are in line with the trend of the results communicated in previous studies and are thus confirmed, as a method of approach and statistical accuracy.

CONCLUSIONS

Imaging analysis based on MSAVI2 and NDVI indices, calculated from satellite images, the PlanetScope product, facilitated the analysis and prediction of barley production under conditions of statistical accuracy. The values of the MSAVI2 and NDVI indices expressed a spatial and temporal variability at the level of the four analyzed barley plots, quantified by means of the coefficient of variation (CV). From the analysis of the prediction errors of the barley production, in relation to the four crop plots and the 7 moments of taking over the images, the plot and the moment were identified in the conditions under which the most accurate prediction was obtained (B/A80, t4).

REFERENCES

Ali, A., Martelli, R., Lupia, F., Barbanti, L. (2019) Assessing multiple years' spatial variability of crop yields using satellite vegetation indices. Remote Sensing, 11 (20), 2384.
DOI: https://doi.org/10.3390/rs11202384

Brogi, C., Huisman, J. A., Herbst, M., Weihermüller, L., Klosterhalfen, A., Montzka, C., Reichenau, T. G., Vereecken, H. (2020) Simulation of spatial variability in crop leaf area index and yield using agroecosystem modeling and geophysics-based quantitative soil information. Vadose Zone Journal, 19 (1), e20009.
DOI: https://doi.org/10.1002/vzj2.20009

Bu, H., Sharma, L. K., Denton, A., Franzen, D. W. (2017) Comparison of satellite imagery and ground-based active optical sensors as yield predictors in sugar beet, spring wheat, corn, and sunflower. Agronomy Journal, 109 (1), 299-308.
DOI: https://doi.org/10.2134/agronj2016.03.0150

Cammarano, D., Zha, H., Wilson, L., Batchelor, W. D., Miao, Y. (2020) A remote sensing-based approach to management zone delineation in small scale farming systems. Agronomy, 10 (11), 1767.
DOI: https://doi.org/10.3390/agronomy10111767

ESRI 2011. ArcGIS Desktop: Release 10. Redlands, CA: Environmental Systems Research Institute.

Galieni, A., D'Ascenzo, N., Stagnari, F., Pagnani, G., Xie, Q., Pisante, M. (2021) Past and future of plant stress detection: An overview from remote sensing to positron emission tomography. Frontiers in Plant Science, 11, 609155.
DOI: https://doi.org/10.3389/fpls.2020.609155

García, M. A., Yagüe, J. L., de Nicolás, V. L., Díaz-Puente, J. M. (2020) Characterization of Globally Important Agricultural Heritage Systems (GIAHS) in Europe. Sustainability, 12 (4), 1611.
DOI: https://doi.org/10.3390/su12041611

Geng, L., Che, T., Ma, M., Tan, J., Wang, H. (2021) Corn biomass estimation by integrating remote sensing and long-term observation data based on machine learning techniques. Remote Sensing, 13, 2352. DOI: https://doi.org/10.3390/rs13122352

Gómez, D., Salvador, P., Sanz, J., Casanova, J. L. (2019) Potato yield prediction using machine learning techniques and Sentinel 2 Data. Remote Sensing, 11 (15), 1745.
DOI: https://doi.org/10.3390/rs11151745

Hammer, Ø., Harper, D. A. T., Ryan, P. D. (2001) PAST: Paleontological statistics software package for education and data analysis. Palaeontologia Electronica, 4 (1), 1-9.

Hansen, P. M., Jørgensen, J. R., Thomsen, A. (2002) Predicting grain yield and protein content in winter wheat and spring barley using repeated canopy reflectance measurements and partial least squares regression. The Journal of Agricultural Science, 139 (3), 307-318. DOI: https://doi.org/10.1017/S0021859602002320

Hkurunziza, L., Watson, C. A., Öborn, I., Smith, H. G., Bergkvist, G., Bengtsson, J. (2020) Socio-ecological factors determine crop performance in agricultural systems. Scientific Reports, 10, 4232.
DOI: https://doi.org/10.1038/s41598-020-60927-1

Jeffries, G. R., Griffin, T. S., Fleisher, D. H., Naumova, E. N., Koch, M., Wardlow, B. D. (2020) Mapping sub-field maize yields in Nebraska, USA by combining remote sensing imagery, crop simulation models, and machine learning. Precision Agriculture, 21 (3), 678-694.
DOI: https://doi.org/10.1007/s11119-019-09689-z

Ji, Z., Pan, Y., Zhu, X., Wang, J., Li, Q. (2021). Prediction of crop yield using phenological information extracted from remote sensing vegetation index. Sensors (Basel, Switzerland), 21 (4), 1406.
DOI: https://doi.org/10.3390/s21041406

Joshi, V. R., Thorp, K. R., Coulter, J. A., Johnson, G. A., Porter, P. M., Strock, J. S., y Garcia, A. G. (2019) Improving site-specific maize yield estimation by integrating satellite multispectral data into a crop model. Agronomy, 9 (11), 719. DOI: https://doi.org/10.3390/agronomy9110719

Jurišić, M., Radočaj, D., Šiljeg, A., Antonić, O., Živić, T. (2021) Current status and perspective of remote sensing application in crop management. Journal of Central European Agriculture, 22 (1), 156-166. DOI: https://doi.org/10.5513/JCEA01/22.1.3042

Kaur, G., Singh, G., Motavalli, P. P., Nelson, K. A., Orlowski, J. M., Golden, B. R. (2020) Impacts and management strategies for crop production in waterlogged or flooded soils: A review. Agronomy Journal, 112 (3), 1475-1501. DOI: https://doi.org/10.1002/agj2.20093

Kefauver, S. C., Vicente, R., Vergara-Díaz, O., Fernandez-Gallego, J. A., Kerfal, S., Lopez, A., Melichar, J. P. E., Serret Molins, M. D., Araus, J. L. (2017) Comparative UAV and field phenotyping to assess yield and nitrogen use efficiency in hybrid and conventional barley. Frontiers in Plant Science, 8, 1733. DOI: https://doi.org/10.3389/fpls.2017.01733

Khalil, Z. H., Abdullaev, S. M. (2021) Neural network for grain yield predicting based multispectral satellite imagery: comparative study. Procedia Computer Science, 186, 269-278. DOI: https://doi.org/10.1016/j.procs.2021.04.146

Khanal, S., Kushal, K. C., Fulton, J. P., Shearer, S., Ozkan, E. (2020) Remote sensing in agriculture - Accomplishments, limitations, and opportunities. Remote Sensing, 12 (22), 3783. DOI: https://doi.org/10.3390/rs12223783

Kumar, L., Sinha, P., Taylor S., Alqurashi A. F. (2015) Review of the use of remote sensing for biomass estimation to support renewable energy generation. Journal of Applied Remote Sensing, 9 (1), 097696. DOI: https://doi.org/10.1117/1.JRS.9.097696

Langridge, P. (2018) Economic and Academic Importance of Barley. In: Stein N., Muehlbauer G. (eds) The Barley Genome. Compendium of Plant Genomes. Springer, Cham. pp. 1-10. DOI: https://doi.org/10.1007/978-3-319-92528-8_1

Maimaitijiang, M., Sagan, V., Sidike, P., Hartling, S., Asposito, F., Fritschi, F. B. (2020) Soybean yield prediction from UAV using multimodal data fusion and deep learning. Remote Sensing of Environment, 237, 111599. DOI: https://doi.org/10.1016/j.rse.2019.111599

Meroni, M., Marinho, E., Sghaier, N., Verstrate, M. M., Leo, O. (2013) Remote sensing based yield estimation in a stochastic framework - Case study of durum wheat in Tunisia. Remote Sensing, 5 (2), 539-557. DOI: https://doi.org/10.3390/rs5020539

Miner, G. L., Delgado, J. A., Ippolito, J. A., Stewart, C. E. (2020) Soil health management practices and crop productivity. Agricultural & Environmental Letters, 5 (1), e20023. DOI: https://doi.org/10.1002/ael2.20023

Mourad, R., Jaafar, H., Anderson, M., Gao, F. (2020) Assessment of Leaf Area Index Models using harmonized Landsat and Sentinel-2 surface reflectance data over a semi-arid irrigated landscape. Remote Sensing, 12 (19), 3121. DOI: https://doi.org/10.3390/rs12193121

Mulla, D. (2021) Trends in satellite remote sensing for precision agriculture. Crops & Soils, 51 (1), 3-5. DOI: https://doi.org/10.1002/crso.20093

Mzid, N., Cantore, V., De Mastro, G., Albrizio, R., Sellami, M. H., Todorovic, M. (2020) The application of ground-based and satellite remote sensing for estimation of bio-physiological parameters of wheat grown under different water regimes. Water, 12 (8), 2095. DOI: https://doi.org/10.3390/w12082095

Newton, A. C., Flavell, A. J., George, T. S., Leat, P., Mullholland, B., Ramsey, L., Revoredo-Giha, C., Rusell, J., Steffenson, B. J., Swanston, J. S., Thomas, W. T. B., Waugh, R., White, P. J., Bingham, I. J. (2011) Crops that feed the world 4. Barley: a resilient crop? Strengths and weaknesses in the context of food security. Food Security, 3, 141. DOI: https://doi.org/10.1007/s12571-011-0126-3

Nguyen, C. T., Chidthaisong, A., Kieu Diem, P., Huo, L. Z. (2021) A Modified Bare Soil Index to Identify Bare Land Features during agricultural fallow-period in Southeast Asia using Landsat 8. Land, 10, 231. DOI: https://doi.org/10.3390/land10030231

Noureldin, N. A., Aboelghar, M. A., Saudy, H. S., Ali, A. M. (2013) Rice yield forecasting models using satellite imagery in Egypt. The Egyptian Journal of Remote Sensing and Space Science, 16, 1, 125-131. DOI: https://doi.org/10.1016/j.ejrs.2013.04.005

Nuruzzaman Manik, S. M., Pengilley, G., Dean, G., Field, B., Shabala, S., Zhou, M. (2019) Soil and crop management practices to minimize the impact of waterlogging on crop productivity. Frontiers in Plant Science, 10, 140. DOI: https://doi.org/10.3389/fpls.2019.00140

Panek, E., Gozdowski, D. (2020) Analysis of relationship between cereal yield and NDVI for selected regions of Central Europe based on MODIS satellite data. Remote Sensing Applications: Society and Environment, 17, 100286. DOI: https://doi.org/10.1016/j.rsase.2019.100286

Paudel, D., Boogaard, H., de Wit, A., Janssen, S., Osinga, S., Pylianidis, C., Athanasiadis, I.N. (2021) Machine learning for large-scale crop yield forecasting. Agricultural Systems, 187, 103016. DOI: https://doi.org/10.1016/j.agsy.2020.103016

Planet Labs PBC, www.planet.com (Accesed on 08 October 2021)

Qi, J., Chehbouni, A., Huete, A. R., Keer, Y. H., Sorooshian, S. (1994) A modified soil vegetation adjusted index. Remote Sensing of Environment, 48 (2), 119-126. DOI: https://doi.org/10.1016/0034-4257(94)90134-1

Rouse, J. W., Haas, R. H., Schell, J. A., Deering, D. W. (1973) Monitoring vegetation systems in the Great Plains with ERTS, Third ERTS Symposium, NASA, 1973, SP-351 I, 309-317.

Sakellariou, M., Mylona P. V. (2020) New uses for traditional crops: The case of barley biofortification. Agronomy, 10 (12), 1964. DOI: https://doi.org/10.3390/agronomy10121964

Śatir, O., Berberoglu S. (2016) Crop yield prediction under soil salinity using satellite derived vegetation indices. Field Crops Research, 192, 134-143. DOI: https://doi.org/10.1016/j.fcr.2016.04.028

Shahhosseini, M., Hu G., Huber I., Archontoulis S. V. (2021) Coupling machine learning and crop modeling improves crop yield prediction in the US Corn Belt. Scientific Reports, 11, 1606. DOI: https://doi.org/10.1038/s41598-020-80820-1

Sharifi, A. (2020) Remotely sensed vegetation indices for crop nutrition mapping. Journal of the Science of Food and Agriculture, 100 (14), 5191-5196. DOI: https://doi.org/10.1002/jsfa.10568

Sharifi, A. (2021) Yield prediction with machine learning algorithms and satellite images. Journal of the Science of Food and Agriculture, 101 (3), 891-896. DOI: https://doi.org/10.1002/jsfa.10696

Sharma, P. C., Datta, A., Yadav, A. K., Choudhary, M., Jat, H. S., McDonald, A. (2019) Effect of crop management practices on crop growth, productivity and profitability of rice–wheat system in Western Indo-Gangetic Plains. Proceedings of the National Academy of Science, India Section B: Biological Sciences, 89, 715-727. DOI: https://doi.org/10.1007/s40011-018-0985-x

Shiferaw, B., Smale, M., Braun, H. -J., Duveiller, E., Reynolds, M., Muricho, G. (2013) Crops that feed the world 10. Past successes and future challenges to the role played by wheat in global food security. Food Security, 5, 291-317. DOI: https://doi.org/10.1007/s12571-013-0263-y

Shiu, Y. -S., Chuang, Y. -C. (2019) Yield estimation of paddy rice based on satellite imagery: Comparison of global and local regression models. Remote Sensing, 11 (2), 111. DOI: https://doi.org/10.3390/rs11020111

Sishodia, R. P., Ray, R. L., Singh, S. K. (2020) Applications of remote sensing in precision agriculture: A review. Remote Sensing, 12 (19), 3136. DOI: https://doi.org/10.3390/rs12193136

Spiertz, H. (2013) Challenges for crop production research in improving land use, productivity and sustainability. Sustainability, 5, 1632-1644. DOI: https://doi.org/10.3390/su5041632

Tan, C., Zhou, X., Zhang, P., Wang, Z., Wang, D., Guo, W., Yun, F. (2020) Predicting grain protein content of field-grown winter wheat with satellite images and partial least square algorithm. PloS ONE, 15 (3), e0228500. DOI: https://doi.org/10.1371/journal.pone.0228500

Tedese, T., Senay, G. B., Berhan, G., Regassa, T., Beyene, S. (2015) Evaluating a satellite-based seasonal evapotranspiration product and identifying its relationship with other satellite-derived products and crop yield: A case study for Ethiopia. Internatinal Journal of Applied Earth Observation and Geoinformation, 40, 39-54. DOI: https://doi.org/10.1016/j.jag.2015.03.006

Trepos, R., Champolivier, L., Dejoux, J. -F., Bitar, A. A., Casadebaig, P., Debaeke, P. (2020) Forecasting sunflower grain yield by assimilating leaf area index into a crop model. Remote Sensing, 12 (22), 3816. DOI: https://doi.org/10.3390/rs12223816

Ulfa, F., Orton, T. G., Dang, Y. P., Menzies, N. W. (2022) Developing and testing remote-sensing indices to represent within-field variation of wheat yields: Assessment of the variation explained by simple models. Agronomy, 12, 384. DOI: https://doi.org/10.3390/agronomy12020384

Van Klompenburg, T., Kassahun, A., Catal C. (2020) Crop yield prediction using machine learning: A systematic literature review. Computers and Electronics in Agriculture, 177, 105709. DOI: https://doi.org/10.1016/j.compag.2020.105709

Vuolo, F., Essl, L., Atzverger, C. (2015) Costs and benefits of satellite-based tools for irrigation management. Frontiers in Environmental Science, 3 (52). DOI: https://doi.org/10.3389/fenvs.2015.00052

Wagner, N. C., Maxwell, B. D., Taper, M. L., Rew, L. J. (2007) Developing an empirical yield-prediction model based on wheat and wild oat (Avena fatua) density, nitrogen and herbicide rate, and growing-season precipitation. Weed Science, 55 (6), 652-664. DOI: https://doi.org/10.1614/WS-05-018.1

Wolfram Alpha (2020) Wolfram Research, Inc., Mathematica, Version 12.1, Champaign, IL.

Xue, J., Su, B. (2017) Significant remote sensing vegetation indices: A review of developments and applications. Journal of Sensors, 2017, 1353691. DOI: https://doi.org/10.1155/2017/1353691

Zhang, P. -P., Zhou, X. -X., Wang, Z. -X., Mao, W., Li, W. -X., Yun, F., Guo, W. -S., Tan, C. -W. (2020) Using HJ-CCD image and PLS algorithm to estimate the yield of field-grown winter wheat. Scientific Reports, 10, 5173. DOI: https://doi.org/10.1038/s41598-020-62125-5

Zhao, Y., Potgieter, A. B., Zhang, M., Wu, B., Hammer, G. L. (2020) Predicting wheat yield at the field scale by combining high-resolution Sentinel-2 satellite imagery and crop modelling. Remote Sensing, 12 (6), 1024. DOI: https://doi.org/10.3390/rs12061024

Zhu, X., Guo, R., Liu, T., Xu, K. (2021) Crop yield prediction based on agrometeorological indexes and remote sensing data. Remote Sensing, 13, 2016. DOI: https://doi.org/10.3390/rs13102016